Strain Driven Growth of Zinc Oxide Nanowires on Sapphire:

Controlling Horizontal vs. Standing Growth

B. Nikoobakht[*] and S. Eustis[**]

[*]National Institute of Standards and Technology
100 Bureau Dr. Stop 8372, Gaithersburg, MD 20899, babakn@nist.gov
[**] Directed Vapor Technologies International, Inc., 2 Boar's Head Lane,
Charlottesville, VA 22903, susie.eustis@gmail.com

ABSTRACT

Recently we showed large scale fabrication of field-effect transistors from horizontal ZnO nanowires (NWs) on *a*-plane sapphire. In growth of horizontal ZnO NWs, the substrate experiences a compressive strain of ≈ 7% in its $[0001]_{sap}$ direction (along the width of a NW) to minimize its lattice mismatch with the ZnO NW. Accordingly, ZnO expands along its width to improve its lattice match with the sapphire. Although this system is a highly mismatched one, our results show that horizontal ZnO nanowires grow semicoherently with much fewer misfit dislocations than theoretically expected. We attribute the formation of fewer dislocations to partial strain relaxation of zinc oxide NW to sapphire surface. A critical nanowire thickness is defined beyond which misfit energy largely relaxes to dislocations, changing the growth mode from horizontal to standing.

Keywords: nanowire, TEM cross-sectioning, lattice strain, electron microscopy, focused ion beam.

1 INTRODUCTION

The processes that guide and control "zero"- and one-dimensional (1D) growth of nanocrystals on solid surfaces have been of great interest in the past two decades. The motivation is the possible technological applications of such structures in ongoing miniaturization of optoelectronics and sensing devices [1, 2]. In this direction, 1D nanocrystals or NWs are shown to have potential applications in electrically driven nanodevices [3]. In our previous study, horizontal ZnO NWs were grown from gold nanodroplets using the vapor-liquid-solid (VLS) mechanism [4]. In this process, despite other in-plane growth methods, gold nanodroplets remain the active site in elongation of NWs. We have used this effect to selectively grow ZnO NWs at designated locations and developed a method for large scale fabrication of NW field-effect transistors [5]. The *in-situ* NW growth and device assembly was shown to be an advantage of this method for commercial development of nanowire-based devices. This study is part of a larger project to further understand the potential structural changes of the horizontal ZnO NWs due to the aging or electron transport in a device. In the current work, we characterize the ZnO-sapphire interface before electron transport through NWs. We use focused ion beam (FIB) for sample preparation and high resolution transmission electron microscopy (HRTEM) to characterize NW cross-sections, their interface with *a*-plane sapphire and the extent of interface coherency in a lattice mismatched system. We use these results to explain the strained epitaxial growth and its effect on loss of NW growth directionality above a certain thickness. We also propose a mechanism for change in the growth mode from horizontal to standing.

2 EXPERIENTAL

- *Growth of horizontal NWs:* Semiconductor NWs and whiskers have been prepared using the VLS mechanism in which metal droplets act as growth sites to produce NWs [6]. Using similar principles, we grow horizontal NWs on single-crystal *a*-plane sapphire surface [4]. Gold features with known positions are made from a photolithographically generated pattern.

–*FIB cross-sectioning:* Using a combination of a focused Ga ion beam and a scanning electron microscope (SEM), electron-transparent cross-sections of horizontally grown NWs on *a*-plane sapphire were prepared.

3 RESULTS AND DISCUSSION

Horizontal ZnO NWs are grown on a gold-patterned sapphire substrate (*a*-plane). The growth, as shown in Figure 1a, is directed and takes place selectively where gold nanodroplets are deposited. A typical membrane containing cross-sections of NWs is attached to a TEM grid and is polished to an electron transparency regime. Profiles of these NWs appear to be semicircular, although in some cases the presence of facets leads to a semi-hexagonal appearance. Figure 1b shows an example. In all the studied cross sections, as well as the one shown in Figure

1b, the sapphire at its interface with ZnO undergoes a deformation that considering its large elastic modulus (403 GPa) indicates a significant stress in its [0003] direction.

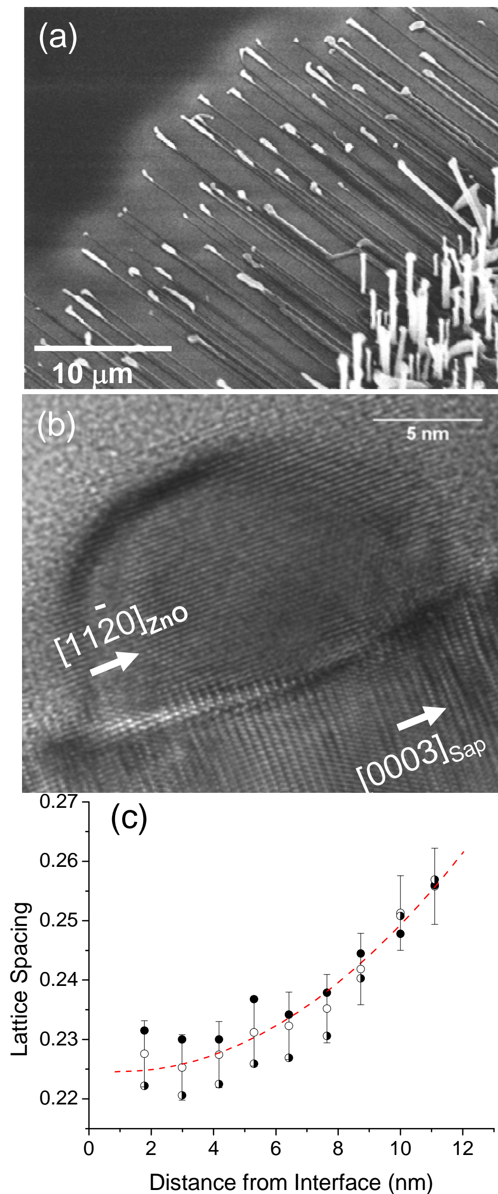

Figure 1. (a) Oriented growth of ZnO NWs, (b) TEM image of a ZnO NW/sapphire cross section. The ZnO **a** and **c** directions are shown with arrows. (c) Illustrates a decrease in the (0002) plane spacing of ZnO by moving from the top to the bottom of the ZnO cross-section. The error bars are ± 0.05 Å, i.e., the uncertainty in the plane spacing measurements.

Due to this stress, sapphire crystal is forced to reconstruct, forming a V-shaped interface with ZnO crystal. The V-shaped interface was more prominent in NWs with diameters less than 15 to 20 nm. For larger diameter NWs the interface curvature appeared more flattened. Previously, high quality epilayers of ZnO were grown on *a*-plane sapphire due to the anisotropic crystal match between the two crystals and the strong tendency of ZnO to grow in c direction [7]. By overlaying c-plane ZnO with *a*-plane sapphire when their **a** and **c** axes are parallel, for every four unit cells of ZnO, the Zn atoms overlap with oxygen atoms of *a*-plane sapphire [5, 7]. The pseudo-lattice match of 99.92 % exists along the length (growth direction) of the NW and is considered to be the main driver in dictating the growth direction of NWs. However, the observed sapphire deformation and reconstruction show that still both crystals try to lower their lattice mismatch and strain in the observed growth. Thus the proposed pseudo-lattice match cannot entirely explain this epitaxial process.

Figure 1b illustrates a ZnO NW cross-section with 18 nm width and 12 nm height. Extension of parallel lattice fringes from sapphire to ZnO crystal is evidence of a crystalline interface. Figure 1c shows that by moving from the top of the ZnO crystal towards the interface, the (0002) plane spacing decreases from 2.53 Å to 2.35 Å. This indicates that the ZnO NW experiences a significant compressive strain of ≤ 7 % in its c direction (normal to the sapphire surface). Based on the Poisson effect, a contraction of ZnO unit cell in the (0002) direction is an indicative of the expansion of the unit cell parallel to the interface. Thus a ZnO nanowire expands along its width, most likely to minimize its lattice mismatch with sapphire. It is important to note that the ZnO planes parallel to the interface were indexed as (0002) because of their observed spacing values. Another possible plane indexing, although unlikely, could be $(10\bar{1}1)$ with a 2.48 Å spacing. Even using this plane assignment, a ZnO NW still experiences a compressive strain in direction normal to the interface.

Based on TEM lattice spacing measurements and crystal plane indexing, the ZnO orientation on sapphire is found to be $(0001)_{ZnO} \parallel (11\bar{2}0)_{Sapp}$ in agreement with our previous electron back-scatter diffraction (EBSD) results [5]. The dominant NW growth direction along the substrate was found to be $(1\bar{1}00)_{ZnO}$.

Sapphire underneath the ZnO NW undergoes changes and demonstrates strain in **c** axis of its unit cell. Depending on the diameter of ZnO NWs, we observe different strain patterns underneath the NWs. For instance, in Figure 2a, sapphire clearly deforms and the V-shape interface appears. Measurements of the sapphire (0003) spacing along the horizontal lines at the bottom of the image show an interesting pattern that is summarized in Figure 2b. There are three regions with different extents of strain that are separated by vertical dashed lines. For the area underneath the ZnO NW (between the vertical dashed lines) spacing ranges from 4.05 Å to 4.15 Å. For the side areas, where sapphire does not have a direct interface with ZnO, d(0003) ranges from 4.33 Å to 4.53 Å. These values are compared with d(0003) of the unstrained sapphire, which are shown with blue stars and measured from sapphire cross-sections. For the middle section, results show that a maximum of 6.9 % compressive strain is created underneath the NW. Using

NSTI-Nanotech 2009, www.nsti.org, ISBN 978-1-4398-1782-7 Vol. 1, 2009

the elastic modulus of bulk sapphire (403 GPa), this lattice strain translates to a maximum compressive stress of ≤ 24 GPa (1GPa = 1nN nm^{-2}).

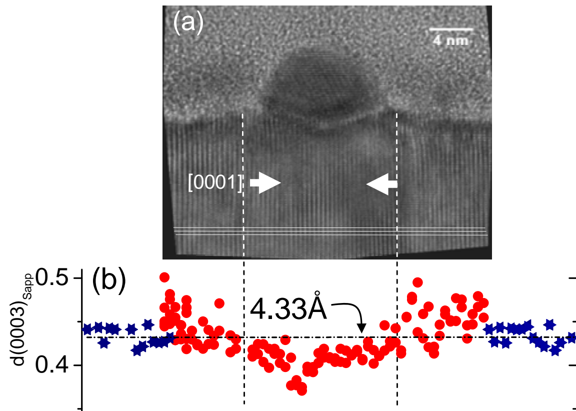

Figure 2. (a) Based on lattice spacing measurements, three vertical sections with different strain patterns can be identified. (b) Strain pattern observed in [0001] direction of sapphire along the NW width.

For the side regions of the interface, a maximum of 5 % tensile stress is observed that gradually decreases toward the middle region. Contribution of strain due to different thermal expansions of ZnO and sapphire is estimated to be about ≈ 0.03 % much lower than the strain observed (supporting information). Overall, the created strain leads to a compression of the sapphire underneath the NW in the direction parallel to the interface, i.e., $[0003]_{sapp}$. As it was pointed out earlier, the ZnO unit cell expands in this direction ($[11\bar{2}0]_{ZnO}$), which leads to a lower lattice mismatch between the two crystals.

In a lattice mismatched system with high interface energy, such as the current case, crystal growth may be accompanied by the formation of misfit dislocations at the interface. Dislocation formation is a mechanism that the overgrown layer undergoes to relax its strain and thus reduce its elastic energy [8]. Alternatively, some of the strain energy could be locally relaxed to its surrounding substrate without introducing misfit dislocations. The idea of overlayer strain energy relaxation to the substrate was originally proposed for the formation of dislocation free Ge islands on Si surface [9]. The evidence that suggests this mechanism may be occurring in our system is the sapphire deformation underneath the NWs. We examined the extent of the created misfit dislocations in both strained and largely relaxed ZnO NWs using the fast Fourier transform (FFT) and image reconstruction using only the power spectrum intensities for reflections of c-plane sapphire and *a*-plane ZnO. Figure 3a illustrates the misfit dislocations for a NW cross-section (18 nm x 12 nm) that is under strain. Dark and white symbols are dislocations in sapphire and ZnO regions, respectively. Dislocations are more apparent in the sapphire section and located near the sides of the NW cross-section. For a large diameter NW (25 nm x 15 nm) in which the ZnO is largely relaxed to its bulk values, dislocations are closer together and their density is higher, which agrees with the fact that the ZnO crystal is more relaxed.

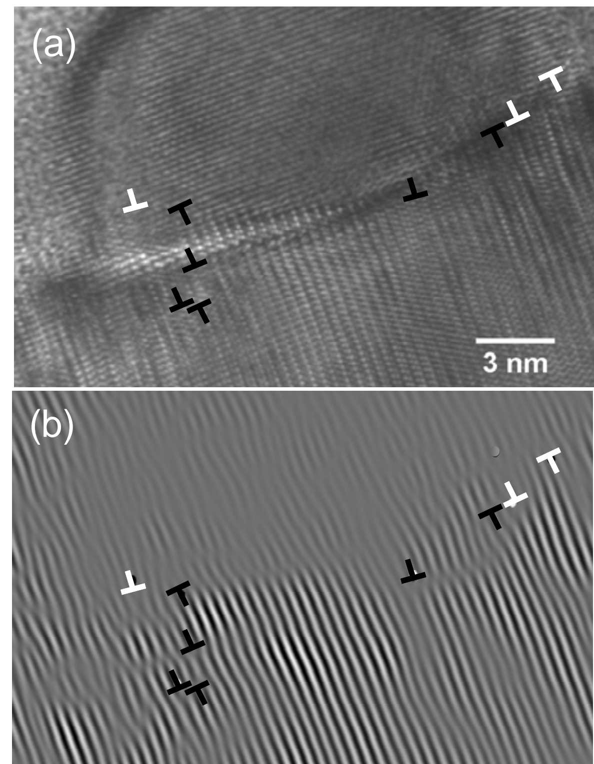

Figure 3. TEM image (a) and its FFT filtered image (b) of cross-section of a strained ZnO. The marked misfit dislocations are located at the edges of the NWs.

The average distance between misfit dislocations of a fully relaxed interface can be calculated using

$$D = (d_1 + d_2)^2/4(d_1 - d_2),$$

where d_1 and d_2 are the lattice spacings for the substrate and the epilayer. For bulk spacing values of ZnO and sapphire, where $d_1 = d(0003)_{Sapp} = 4.33$ Å, and $d_2 = d(11\bar{2}0)_{ZnO} = 1.63$ Å, the expression above generates a value of 3.29 Å for the dislocation spacing; although this value may physically not be reasonable, it corresponds to an incoherent ZnO/sapphire interface [8]. An incoherent interface has no local relaxation of the misfit into dislocations. The misfit is instead spread evenly across the entire interface, where the epilayer and the underlying substrate retain their bulk structures. On the other extreme, for a 0.08 % pseudo-lattice mismatch ZnO/sapphire interface, using the above equation, the spacing between two adjacent misfit dislocations would be 339 nm. The observed dislocation spacings are far from the expected values for both incoherent and coherent interfaces. In

addition, *a*-plane sapphire at its interface with ZnO reconstructs to planes with higher index as a mechanism to decrease its lattice mismatch with ZnO. These all indicate that ZnO NW holds a level of semicoherency on *a*-plane sapphire and its strain energy is not fully relaxed to misfit dislocations. It also supports the suggestion above that some of the ZnO strain energy is locally relaxed to the sapphire substrate causing its deformation underneath the ZnO NW.

Although in NW growth, individual islands are not formed, elongation of a horizontal NW is considered as a sequential island growth in one direction. At any point of time, a gold nanodroplet provides the confined volume for growth of a portion of a ZnO NW. In promoting the horizontal growth, we think, an important factor is coexistence of a gold interface with both ZnO and sapphire during the entire growth period of a NW, which is schematically shown in Figure 4a.

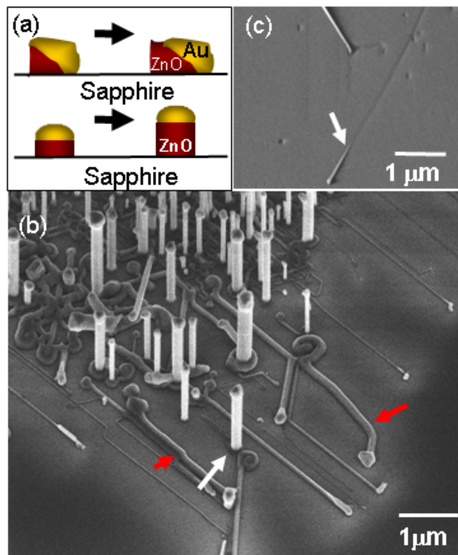

Figure 4. (a) Top part, shows two stages of growth of a horizontal NW. It also shows the three necessary interfaces to have such a growth. (b-c) SEM images of different growth modes of ZnO NWs.

The existence of this ternary interface is dependent on the ZnO crystal thickness. Our results imply that wetting of ZnO by gold nanodroplet becomes dependent on the ZnO crystal size. Above a nanodroplets critical thickness of ≈ 25 nm, the ternary interface of gold/sapphire/ZnO reduces to only a gold/ZnO interface, which causes gold to only wet the ZnO crystal. This leaves one choice for NW and that is to grow in a standing (off-plane) fashion, as marked by white arrows in Figures 4(b-c). Another factor that is coupled with the mechanism above is the extent of formation of misfit dislocations and interface energy of ZnO/sapphire. We think for ZnO NWs above the critical diameter of ≈ 25 nm, the strain energy reaches a limit where relaxation through formation of misfit dislocations becomes favorable. The increase in the number of misfit dislocations increases the misfit energy of the interfacial free energy of ZnO/sapphire thus decreasing the adhesion energy between ZnO and sapphire crystals. Indeed, in our previous study of cross-section of *standing* ZnO NWs, we have observed misfit dislocations for NWs with diameters more than 50 nm [10]. At this size regime, the sapphire substrate gradually loses its dictate over horizontal NW growth direction. Such a poor growth directionality has been observed for horizontal NWs grown from gold nanodroplets larger than ≈ 25 nm and an example is shown in Figure 4c (red arrows).

4 CONCLUSIONS

The studied system is a highly lattice mismatched one; however, horizontal ZnO nanowires grow semicoherently. Examining the interface shows fewer misfit dislocations than theoretically expected, which agrees with the observed lattice strain in both ZnO and Sapphire. The strain in ZnO decreases as width of the NW increases; a fact that is in accord with the formation of more misfit dislocations at the interface. This also agrees with the fact that thicker NWs tend to grow out of substrate plane. Depending on the diameter of the grown NWs three growth regimes are evident: thick NWs, displaying a standing growth mode; small diameter NWs, showing an in-plane oriented growth mode; and a state in-between, where the growth directionality is poor. It is the ZnO and sapphire *interaction* that determines the fate of the growth direction. However, it is the gold nanodroplet *partial* wetting of both crystals that makes the gold nanodroplet a "mobile" crystal grower on sapphire surface directing the transition from horizontal to vertical growth.

REFERENCES

[1] Goldhaber-Gordon, D.; Monterelo, M. S.; Love, J. C.; Opiteck, G. J.; Ellenbogen, J. C. *Proc. IEEE*, **1997**, *85*, 521–540.
[2] Bimberg, D. *Semiconductors*, **1999**, *33*, 951–955..
[3] Duan, X.; Huang, Y.; Agarwal, R.; Lieber, C. M. *Nature*, **2003**, *421*, 241-245.
[4] Nikoobakht, B.; Michaels, C. A.; Vaudin, M. D.; Stranick, S. J. *Appl. Phys. Lett.* **2004**, *85*, 3244-3246.
[5] Nikoobakht, B. *Chem. Mater.* **2007**, *19*, 5279-5284.
[6] Huang, M. H.; Wu, Y.; Feick, H.; Tran, N. Weber, E.; Yang, P. *Adv. Mater.* **2001**, *13*, 113-116.
[7] Fons, P.; Iwata, K.; Yamada, A.; Matsubara, K.; Niki, S.; Nakahara, K.; Tanabe, T.; Takasu, H. *App. Phys. Lett.* **2000**, *77*, 1801-1803.
[8] Frank, F. C.; Van der Merwe, J. H. *Proc. Roy. Soc. London* A **1949**, *198*, 205-216.
[9] Eaglesham, D. J.; Cerullo, M. Dislocation-Free Stranski-Krastanow Growth of Ge on Si (100). *Phys. Rev. Lett.* **1990**, *64*, 1943.
[10] Levin, I.; Davydov, A.; Nikoobakht, B.; Sanford, N. Mogilevsky, P. *Appl. Phys. Lett.* **2005**, *87*, 1031101.

NSTI-Nanotech 2009, www.nsti.org, ISBN 978-1-4398-1782-7 Vol. 1, 2009